X-ray and NMR Characterization of Covalent Complexes of Trypsin, Borate, and Alcohols

Thomas R. Transue, Joseph M. Krahn, Scott A. Gabel, Eugene F. DeRose, and Robert E. London*

Laboratory of Structural Biology, National Institute of Environmental Health Sciences, National Institutes of Health, 111 T.W. Alexander Drive, Research Triangle Park, North Carolina 27709

Received October 2, 2003; Revised Manuscript Received December 5, 2003

ABSTRACT: An understanding of the physiological and toxicological properties of borate and the utilization of boronic acids in drug development require a basic understanding of borate-enzyme chemistry. We report here the extension of our recent NMR studies indicating the formation of a ternary borate−alcohol−trypsin complex. Crystallographic and solution state NMR studies of porcine trypsin were performed in the presence of borate and either of three alcohols designed to bind to the S1 affinity subsite: 4-aminobutanol, guanidine-3-propanol, and 4-hydroxymethylbenzamidine. Quaternary complexes of trypsin, borate, S1-binding alcohol, and ethylene glycol (a cryoprotectant), as well as a ternary trypsin, borate, and ethylene glycol complex have been observed in the crystalline state. Borate forms ester bonds to Ser195, ethylene glycol (two bonds), and the S1-binding alcohol (if present). Spectra from ^{1}H and ^{11}B NMR studies confirm that these complexes also exist in solution and also provide evidence for the formation of ternary trypsin, borate, and S1-subsite alcohol complexes which are not observed in the crystals using our experimental protocols. Analysis of eight crystal structures indicates that formation of an active site borate complex is in all cases accompanied by a significant (∼4%) increase in the *b*-axis dimension of the unit cell. Presumably, our inability to observe the ternary complexes in the crystalline state arises from the lower stability of these complexes and consequent inability to overcome the constraints imposed by the lattice contacts. A mechanism for the coupling of the lattice contacts with the active site that involves a conformational rearrangement of Gln192 is suggested. The structures presented here represent the first crystallographic demonstration of covalent binding of an enzyme by borate.

Boric acid has a wide range of industrial applications and is a common constituent of insecticides and wood preservatives (*1*). It has been reported to exert a broad range of physiological effects, among the most provocative that it functions as a regulator of the inflammatory response (*2*). Moderate borate levels have also been found to interfere with male reproductive function (*3*). Recent interest in borate compounds has been sparked by studies of 2-aminoethoxydiphenyl borate (2-APB),[1] an inhibitor of store-operated Ca^{2+} channels (*4*, *5*), and by a furanosyl borate diester that appears to function as a universal signal for communication among bacteria (*6*). Boronic acid compounds, and particularly boropeptides, are well-known inhibitors of serine proteases (*7*, *8*), and borate itself weakly inhibits these enzymes (*9*, *10*). An understanding of the physiological and toxicological properties of borate, as well as the exploitation of boronic acid functionality in drug development, require information about the interaction of borate with enzymes and other biological macromolecules.

Biochemical studies of the enzyme γ-glutamyl transpeptidase (γGT) initially reported in 1959 (*11*) led to the proposal that this enzyme could synthesize its own inhibitor by stabilizing a labile ester linkage between L-serine and borate, both bound in the active site. The resulting ternary complex was proposed to function as a mimic of the transition state, with a tetrahedral borate anion linked to the serine Oγ, and to indeterminate residues of the enzyme (*12*). Support for this hypothesis was recently obtained by the construction of an isomeric boronate compound, L-2-amino-4-boronobutanoic acid (ABBA)[1], in which the putative labile ester bond was replaced by a nonlabile methylene−boron bond (*13*, *14*). The successful development of a more selective and potent inhibitor for this enzyme—the K_i of ABBA is more than 4 orders of magnitude lower than an equimolar serine−borate mixture (*15*)—has important implications for the more general development of enzyme inhibitors. Although a structural characterization of the γGT−serine−borate ternary complex would provide the most direct approach for verification of this hypothesis, it has been difficult to obtain structural information for γGT, a membrane-associated enzyme. Further, the above observations have broader implications for the entire class of serine proteases, which are mechanistically related to γGT. Serine proteases fulfill a broad range of biochemical functions, making many of the enzymes in this class attractive drug

* To whom correspondence should be addressed. Robert E. London, MR-01, Laboratory of Structural Biology, NIEHS, Box 12233, Research Triangle Park, NC 27709; e-mail: london@niehs.nih.gov; phone: (919) 541-4879; fax: (919) 541-5707.

[1] Abbreviations: ABBA, L-2-amino-4-borono butanoic acid; EG, ethylene glycol; γGT, γ-glutamyl transpeptidase; G3P, guanidine-3-propanol; 4AB, 4-amino-1-butanol; pHMBA, 4-hydroxymethylbenzamidine.

10.1021/bi035782y
Published on Web 02/18/2004

targets (*7*). For example, these enzymes play important roles in apoptosis (*16*, *17*), bacterial (*18*), and viral (*19*) pathogenesis, neoplasia (*20*−*22*), blood coagulation (*23*), fibrinolysis (*24*), T cell activation (*25*), and complement activation (*26*). Hence, the development of serine protease inhibitors is of considerable practical interest.

We have recently obtained kinetic and NMR evidence for the formation of an analogous ternary complex formed from the enzyme trypsin, borate, and 4-aminobutanol (4AB)[1] with the latter alcohol, a lysine analogue, selected to bind to the S1-subsite of trypsin. In that study, the ^{1}H and ^{11}B NMR data indicate the formation of a complex characterized by covalent bonding of the borate to the hydroxyl oxygen of Ser195 and to the alcohol function of 4AB. The X-ray crystallographic and NMR studies described here were undertaken to obtain more direct evidence for the proposed borate complexes, and represent the first crystallographic evidence for covalent adduct formation involving an enzyme. These observations have important implications for the use of enzymes as active participants in the design of potent and selective inhibitors (*27*−*34*).

MATERIALS AND METHODS

Crystal Preparation. Type IX porcine pancreatic trypsin (Sigma, St. Louis, MO) was dissolved to a final concentration of 30 mg/mL in 100 mM G3P.[1] The pH was adjusted to 8.0 with NaOH, and the stock solution was stored at 4 °C. Initial crystals grew within several days of setup in sitting drop vapor diffusion experiments (2 μL of protein plus 2 or 3 μL of well solution) in which well solutions contained 1.6−1.8 M $MgSO_4$, 50 mM HEPES or Tris (pH 8.0), and 5 mM $CaCl_2$. Boric acid was adjusted to pH 8.0 with NaOH and added to well solutions for final concentrations of 0, 5, 30, and 90 mM; however, no crystals were observed in drops made with 30 or 90 mM borate. Crystals were harvested into solutions containing 2 M $MgSO_4$, 50 mM HEPES (pH 8.0), 50 mM G3P. They were then transferred 4 times to fresh, inhibitor free drops containing 80 μL of 2 M $MgSO_4$, 50 mM HEPES (pH 8.0), and 5 mM $CaCl_2$ over a period of 3 h. The structure of the resulting crystals was solved confirming the absence of S1-subsite inhibitors. These crystals were further soaked into solutions containing either 5 mM *p*HMBA[1] or 100 mM 4AB to produce alternate S1-subsite complexes. To produce trypsin/borate/ethylene glycol (EG) complexes, the above crystals were further soaked in solutions also containing 200 or 250 mM borate (pH 8.0) for 1−20 min and then transferred to an 80:20 (v/v) mixture of the same solution with EG. Crystals were flash frozen in liquid nitrogen. Since, as discussed below, it was found that the use of EG as a cryoprotectant typically resulted in the formation of a quaternary complex, some crystals were transferred to saturated magnesium sulfate, which served as an alternative cryoprotectant.

Data Collection and Refinement. Data were collected using a Rigaku rotating anode generator and R-AXIS IV detectors (Molecular Structure Corporation). Data were reduced with DENZO and SCALEPACK (HKL Research) (*35*). As a starting model, PDB model code 1AKS (*36*) was downloaded and reothogonalized to adjust for slight differences in unit cell dimensions. The starting model backbone was also reconnected after residue K145, and N165D and Q186E sequence changes were made to match the expected porcine pancreatic trypsin sequence. All models were refined using a maximum likelihood target against all intensities using CNS (*37*). Force parameters were taken from the AMBER force field (*38*). All hydrogen atoms were used so as to model their weak but significant contribution to the X-ray scatter and to avoid producing models in which deduced hydrogen positions necessarily cause clashes with each other or with non-hydrogen atoms. Ions Ca^{2+}, Na^{+1}, Mg^{2+}, and SO_4^{-2} were identified based on coordination geometry and distance, ligand type, electron density maps considering the refined occupancy and B-factor, and the known calcium binding site. Alternate conformations were modeled where difference electron density and reasonable hydrogen bond and VDW contacts suggested that two or three conformations would better represent the data. The relative occupancies were chosen to reduce difference density as much as possible. Occupancies of water molecules were refined while manually monitoring free-R factors to avoid overfitting the data. Models and scaled intensity data have been deposited in the PDB (see Table 1 for codes).

NMR Studies. Type IX porcine pancreatic trypsin was obtained from Sigma (St. Louis, MO). Guanidino-3-propanol (G3P) and 4-hydroxymethylbenzamidine (*p*HMBA) were custom synthesized by UNIC, LLC (Research Triangle Park, NC), and 4-aminobutanol (4AB) was obtained from Aldrich (Milwaukee, WI). ^{1}H and ^{11}B NMR spectra were obtained on a Varian Unity 500 NMR spectrometer operating at 160.6 MHz for boron. The ^{1}H spectra were obtained at 5 °C and utilized a jump and return sequence to suppress the H_2O resonance (*39*). The lower temperature was used in the ^{1}H NMR studies to limit the exchange broadening of the imidazole NH proton resonances. The ^{1}H NMR studies also used high (500 mM) borate concentrations to inhibit proteolysis of the trypsin. The ^{11}B studies utilized only 25 mM borate to minimize the complexity arising from nonspecific binding of the borate to potential impurities or to additional sites on the trypsin. Nevertheless, as noted below, we do obtain evidence for additional (non-active site) binding interactions at 25 mM borate. ^{1}H spectral parameters were: sweep width, 16 kHz; acquisition time, 1.0 s; transients, 2000. The ^{11}B spectra were obtained at 25 °C using a 5-mm quartz NMR tube (Wilmad, Buena, NJ) and a 5-mm Nalorac probe (Martinez, CA), which had been modified to reduce the boron background. ^{11}B spectral parameters were sweep width, 10 kHz; acquisition time, 0.6 s; transients, 44 400. ^{11}B shifts are referenced to external boric acid at pH 4.0.

RESULTS

Eight Crystal Structures. Crystals of porcine trypsin were prepared with either a vacant S1-subsite or with the S1-subsite occupied by one of three alcohols, selected for their properties as substrate analogues: guanidine-3-propanol (G3P, an arginine analog), 4-aminobutanol (4AB, a lysine analogue), and *para*-hydroxymethylbenzamidine (*p*HMBA, an analogue of *p*-amidinophenylalanine which has also been incorporated into substrates for trypsin and related enzymes (*40*). Each compound contains a positively charged group on one end and an alcohol function on the other. Each of the resulting four crystal structures was solved, and the presence or absence of substrate analogue was confirmed. Crystals from each of the four conditions were then soaked

in solutions containing borate to form covalent complexes. As discussed further below, EG, used as a cryoprotectant during data collection, fortuitously formed an important part of the covalent complex.

Structural Overview. The trypsin crystals belong to the orthorhombic $P2_12_12_1$ space group, with a single trypsin molecule in each asymmetric unit. The overall structures of the trypsin complexes presented here are very similar to each other as the eight superposed models produce pairwise RMS deviations based on 223 Cα's ranging from 0.10 to 0.41 Å. Likewise, when the eight models are superposed with the starting model used for molecular replacement (PDB code 1AKS[20]), the RMS deviations from 223 Cα's range from 0.28 to 0.39 Å. Figure 1 illustrates the active sites where the most significant differences between the eight structures are seen. On the left side (Figure 1a,c,e,g), the four structures lacking borate are shown. Each structure can be compared with its counterpart on the right side (Figure 1, panels b, d, f, and h, respectively) in which borate forms a covalent adduct with the active site Ser195 hydroxyl group. In each of these cases, the two hydroxyl groups of the EG cryoprotectant substitute for two of the remaining three hydroxyl groups on the borate. The fourth borate hydroxyl group is free (Figure 1b) or substituted by the alcohol function of the substrate analogue bound to the S1-subsite (Figure 1d,f,h). Evidently, the flexibility of the serine/borate linkage allows a covalent bond to form with the substrate analogue without disrupting its binding.

Binding Site. A detailed look at S1-subsite and active site residues reveals which ones appear unchanged and which must rearrange to accommodate the borate binding. In the S1-subsite, Asp189 is positioned to balance the positive charge of the incoming substrate lysine or arginine. In the structures presented here, Asp189 coordinates the G3P guanidinium group and the *p*HMBA amidino group directly (Figure 1c,d,g,h), while the 4AB amino group makes contact to Asp189 through a bridging water molecule (Figure 1e,f). When no substrate analogue is present, a solvent EG molecule occupies part of the S1-subsite and Asp189 coordinates a sodium ion identified based on its coordinating neighbors, distances, and geometry (Figure 1a,b). Despite the varied contacts that Asp189 makes in these structures, the similarity with which the carboxylate side chain aligns when all eight structures are superposed suggests that the residue is well anchored in the trypsin structure. Even when the alcohol adopts two distinct alternate conformations (Figure 1c), the side chain is well ordered and refines with relatively low B-factors. With generally little variation, Ser190 and several other residues not shown in Figure 1 also help to coordinate the occupant of the S1-subsite with both side chain and main chain hydrogen bond and van der Waals contacts. More detailed presentations of the active site electron densities are included as Supporting Information. On the other end of the S1-subsite, Ser195, His57, and Asp102 (chymotrypsin numbering used throughout) form the catalytic triad of this serine protease. In each structure (Figure 1a−h), Asp102 accepts a hydrogen bond from His57. When a substrate analogue is noncovalently bound in the S1-subsite (Figure 1c,e,g), Ser195 accepts a hydrogen bond from His57 and donates a hydrogen bond to the alcohol function present on each substrate analogue. When no substrate analogue is present (Figure 1a), the Ser195 hydroxyl donates a hydrogen bond to a solvent EG molecule occupying part of the S1-subsite. In addition, the hydrogen bond donated by His57 is stretched to 3.4 Å, and also is bridged by a water molecule (Figure 1a). In the presence of borate and EG, Ser195 is seen covalently bonded to the tetrahedral borate anion. The EG molecule forms a five-membered ring with the boron center (Figure 1b,d,f,h). When compared to the corresponding structures not containing borate, Ser195 adopts a similar rotomer, but the Oγ moves as much as 1 Å toward His57. His57 in turn rotates slightly about the Cα−Cβ bond, moving away from Ser195 and lining up to donate a hydrogen bond to an ester oxygen in the five-membered ring of the borate/EG complex (Figure 1b,d,f,h).

Additional Features of Crystal Structures. Alternate conformations of some parts of the models were observed and modeled in each of the structures presented here. Most of these involve two discrete conformational alternatives with occupancies near 50%. Relevant to discussions of this paper are the two conformations adopted by G3P in the absence of borate/EG. The guanidinium group flips 180 degrees to form different hydrogen bonds with neighboring groups (Figure 1c). Also, the hydroxyl group of *p*HMBA rotates about 120 degrees to form hydrogen bonds with either Ser195 OH or a sulfate ion modeled as being present only 60% of the time. Worth mentioning for their structural significance are the two to three distinct conformations of the disulfide bond between Cys191 and Cys220 (see the upper left corner of Figure 1a−g in Supporting Information).

In addition to active site features, these structures present several other noteworthy characteristics. The covalent binding of borate/EG is associated with a significant change (about 2 Å or almost 4%) in the crystal unit cell *b*-axis. The side chain of Gln192 appears to play an important role in this transition. In the absence of borate, the Gln192 amide group is folded toward the active site (Figure 2). When borate occupies the active site, the side chain extends outward and makes a hydrogen bond with Asn233 in another trypsin molecule related by crystal symmetry. The symmetry-related molecule must move away along the *b*-axis to accommodate the new side chain conformation. Other interactions may also be responsible for favoring the extended *b*-axis, but apparently the lattice contacts readily tolerate this transition when crystals are soaked in borate-containing solutions followed by a 20% EG solution. There is no apparent damage to the crystal, and the change was shown to be reversible by collecting data from a borate/EG-soaked crystal, then thawing the crystal in a saturated $MgSO_4$ solution for 30 s, refreezing, and collecting a second data set. The first structure showed clear presence of the covalent complex and exhibited the larger unit cell b-dimension, while the latter (data not shown) contained no borate and had a ∼2 Å smaller unit cell b-dimension.

Proton and Boron NMR Studies. To compare the crystallographic results with the solution behavior of this system, NMR was used to follow the effects of titration of ethylene glycol into samples initially containing trypsin, borate, and either of the three alcohols 4AB, G3P, or *p*HMBA. Prior to the addition of EG, the ^{11}B NMR spectrum of the trypsin−borate−G3P containing sample exhibits two resonances at −1 and −17.4 ppm corresponding to uncomplexed borate (actually a concentration weighted average due to the boric acid and borate forms of the molecule) and to the borate

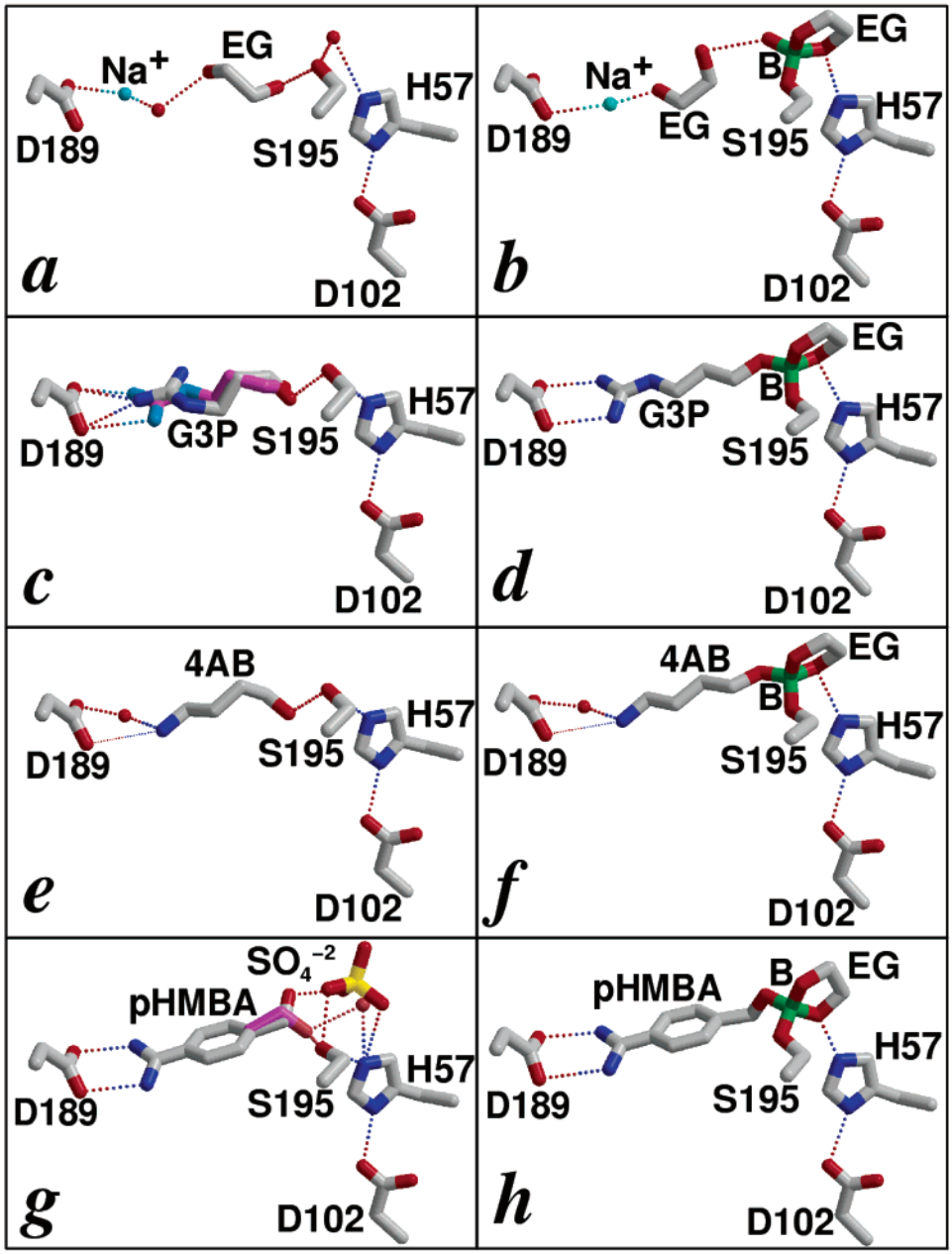

FIGURE 1: Identical views of the active site of porcine trypsin from eight separate crystal structures. Each figure shows the side chains for the three residues of the catalytic triad, His57, Asp102, and Ser195, as well as Asp189 located at the end of the S1 specificity subsite. The positions of the S1-binding alcohols, borate, ethylene glycol, selected water molecules (red spheres), and sodium ions are also indicated. In addition to the use of red and blue color coding of oxygen and nitrogen atoms, respectively, boron is indicated in green, sodium is in cyan, sulfate sulfur is in yellow, and carbon atoms in the alternate positioning of guanidino-3-propanol and *p*-hydroxymethyl benzamidine are tinted purple. (a) No S1-subsite specific inhibitor or borate is present. The S1-subsite is occupied by a sodium ion, a water molecule, and an ethylene glycol molecule which hydrogen bonds to Ser195. (b) No S1-subsite-binding alcohol is present, but borate/EG is covalently bound as indicated. Sodium and free ethylene glycol occupy the S1-subsite, similarly to observations in Figure 1a. (c) The S1-subsite is occupied by G3P which appears to adopt two distinct conformations (X-ray data are consistent with 55% conformation one shown with carbon in white and 45% conformation two shown with carbon in purple). (d) The S1-subsite is occupied by G3P. Borate forms a covalent complex with G3P, EG, and Ser195. Only conformation two from panel c is seen. (e) The S1-subsite is occupied by 4AB. The primary amino group does not make direct H-bond contact with Asp189, but rather a water molecule bridges the opposite charges, and the narrower dotted line indicates a 3.4 Å salt bridge between a Asp189 carboxyl oxygen and the 4AB amino group. (f) The S1-subsite is occupied by 4AB which is part of a covalent complex with borate, EG, and Ser195. The amino group lies 3.3 Å from Asp189 (essentially the same place as in panel e) and interacts through a similarly placed water molecule. The 4AB hydroxyl group, however, shifts to form a covalent bond with the borate. (g) The S1-subsite is occupied by *p*HMBA. Two distinct arrangements are visible (data are consistent with 65% conformation one shown with carbon in white and 35% conformation two shown with carbon in purple). In conformation one, the *p*HMBA hydroxyl group donates a hydrogen bond to a sulfate ion modeled as having 60% occupancy. In conformation two, the hydroxyl group is rotated about 120 deg to form a hydrogen bond with a water molecule with 40% occupancy. (h) The S1-subsite is occupied by *p*HMBA which is covalently bonded to borate, EG, and Ser195. The orientation of *p*HMBA resembles that in panel g, except that compared with the positions seen in panel g, the hydroxyl group (covalently attached to borate) is rotated about 110° from conformation one or about 160° from conformation two.

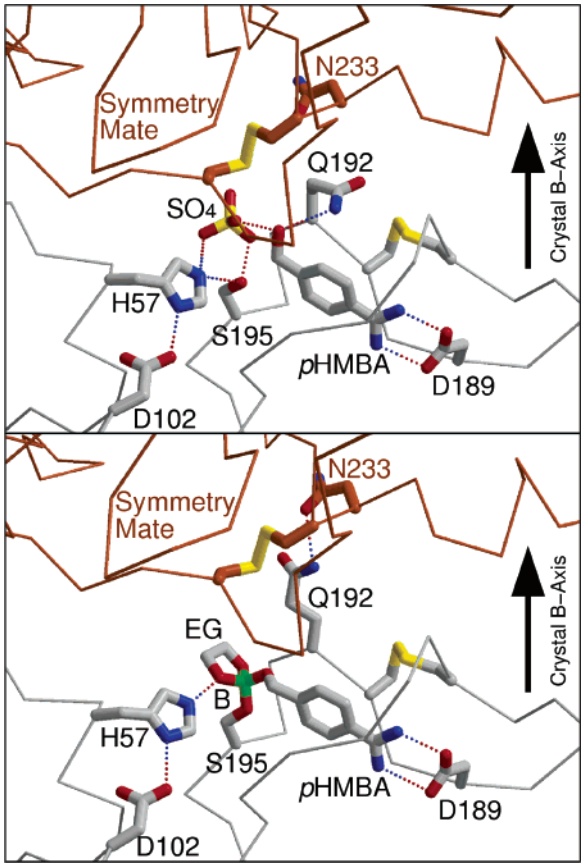

FIGURE 2: Examination of a series of eight trypsin structures indicates that formation of an active site borate−alcohol complex is accompanied by expansion of the crystal parallel to the *b*-axis of the unit cell. The above figure illustrates an α-carbon trace corresponding to the active site of one trypsin molecule (shown in white) and the proximate residues of a symmetry-related molecule (shown in brown). Several of the side chains have been drawn in as well. The upper trace corresponds to the structure shown in Figure 1g, in which pHMBA is bound to the S1-subsite of the enzyme. Side chains corresponding to the residues of the catalytic triad (H57, D102, and S195), D189, Q192, and the disulfide bond connecting C191 and C220 are also indicated. In the lower trace, corresponding to the structure depicted in Figure 1h, formation of the borate complex is shown to be accompanied by a significant change in the conformation of Q192, so that it extends toward the symmetry-related trypsin molecule in a direction that approximately parallels the crystal *b*-axis.

anion bound to the enzyme, respectively (Figure 3a). As in our previous study of the interaction of trypsin with 4AB and borate (*10*), the ^{11}B shift of the bound borate corresponds to a tetrahedral borate anion, which is presumably esterified to the oxygen atoms of both Ser195 and G3P. Addition of EG results in the appearance of an additional resonance at −13.3 ppm, which we assign to the quaternary trypsin/G3P/borate/EG complex observed in the crystalline state (Figure 1d). Successive additions of EG result in further increases in the intensity of the −13.3 ppm peak and to decreases in intensity of the −17.4 ppm peak, corresponding to the gradual conversion of the ternary to the quaternary complex. Qualitatively similar results were obtained in ^{11}B NMR studies using either of the other two alcohols (Figure 3b,c). We note also that in many of the spectra, the resonance identified as the "ternary" complex exhibits an upfield shoulder. This shoulder is not readily observed using 5 mM borate (*10*), but becomes apparent at the higher 25 mM borate concentration used in these studies. On the basis of the observed shift, this resonance arises from a borate complex, and presumably corresponds to an interaction with another site on the trypsin, or to a complex formed with an impurity. The identity of this resonance is currently under investigation.

A parallel ^{1}H NMR examination of the downfield shifted resonances arising from His57 confirms this analysis. The ternary trypsin−borate−G3P complex is characterized by two proton resonances at 15.4 and 16.6 ppm, indicating the imidazolium form of the histidine side chain (Figure 4a). By analogy with the trypsin−boropeptide complexes studied by Tsilikounas et al. (*41*), these resonances are assigned to the labile Hδ1 and Hε2 protons, respectively, on the histidine. Addition of EG results in the appearance of two new resonances at 15.1 and 16.8 ppm, which are assigned to Hδ1 and Hε2, respectively, of the quaternary complex. As in the ^{11}B NMR study discussed above, continued EG addition reduces the signals corresponding to the ternary complex as the signals arising from the quaternary complex increase. Another interesting feature of the spectra shown in Figure 4 is the Hδ1 line width difference observed between the ternary and quaternary complexes. The chemical exchange of Hδ1 in the ternary complex leads to a broad resonance, and limits the observation of 2D NOESY cross-peaks to Hδ1 in this system. However, in the quaternary complex, this resonance sharpens considerably, indicating a more stable structure. Mechanistically, this effect probably arises from the stabilization of the tetrahedral borate coordination imposed by the bidentate ligation of the EG. The ^{1}H NMR spectra obtained from an EG titration study of the trypsin−borate−4AB complex shows a qualitatively similar pattern, both in terms of the shifts and broadening of the Hδ1 resonance (Figure 4b). 2D NOESY experiments performed on the complexes noted above were consistent with the histidine assignments indicated in Figures 4 and 5 but did not provide definitive assignment information.

^{11}B NMR spectra were also obtained for mixtures of borate and ethylene glycol in the absence of trypsin. These spectra are characterized by a broad resonance at −12.3 ppm and a smaller, broad resonance at −10.2 ppm (data not shown). On the basis of the studies of Coddington and Taylor (*42*), these resonances correspond to the EG complexed with borate and triborate ($B_3O_5^{-1}$), respectively. On the basis of the line width, the lifetime of the borate/EG complex is estimated as 0.55 ms. Addition of trypsin led to further broadening of the resonances. Thus, although a ternary trypsin/borate/EG complex may form, the lifetime is considerably shorter than that of the trypsin/S1-binding alcohol/borate complexes observed by NMR. We note that the ^{11}B NMR spectra of the trypsin−borate−alcohol systems obtained at 800 mM EG (Figure 3) also show some evidence of these broad resonances near −10 and −12 ppm, consistent with the assignment of these peaks to borate−EG and trypsin−borate−EG complexes noted above,

In contrast to the results obtained for the 4AB and G3P complexes, the *p*HMBA formed a different type of ternary complex in solution. The ^{1}H NMR spectrum of the His57 protons reveals only a single proton resonance at 15.6 ppm (Figure 4c), rather than the two resonances observed in the other ternary complexes (Figure 4a,b). Analogous observations on related systems have been interpreted to indicate formation of a type II complex, in which the borate or

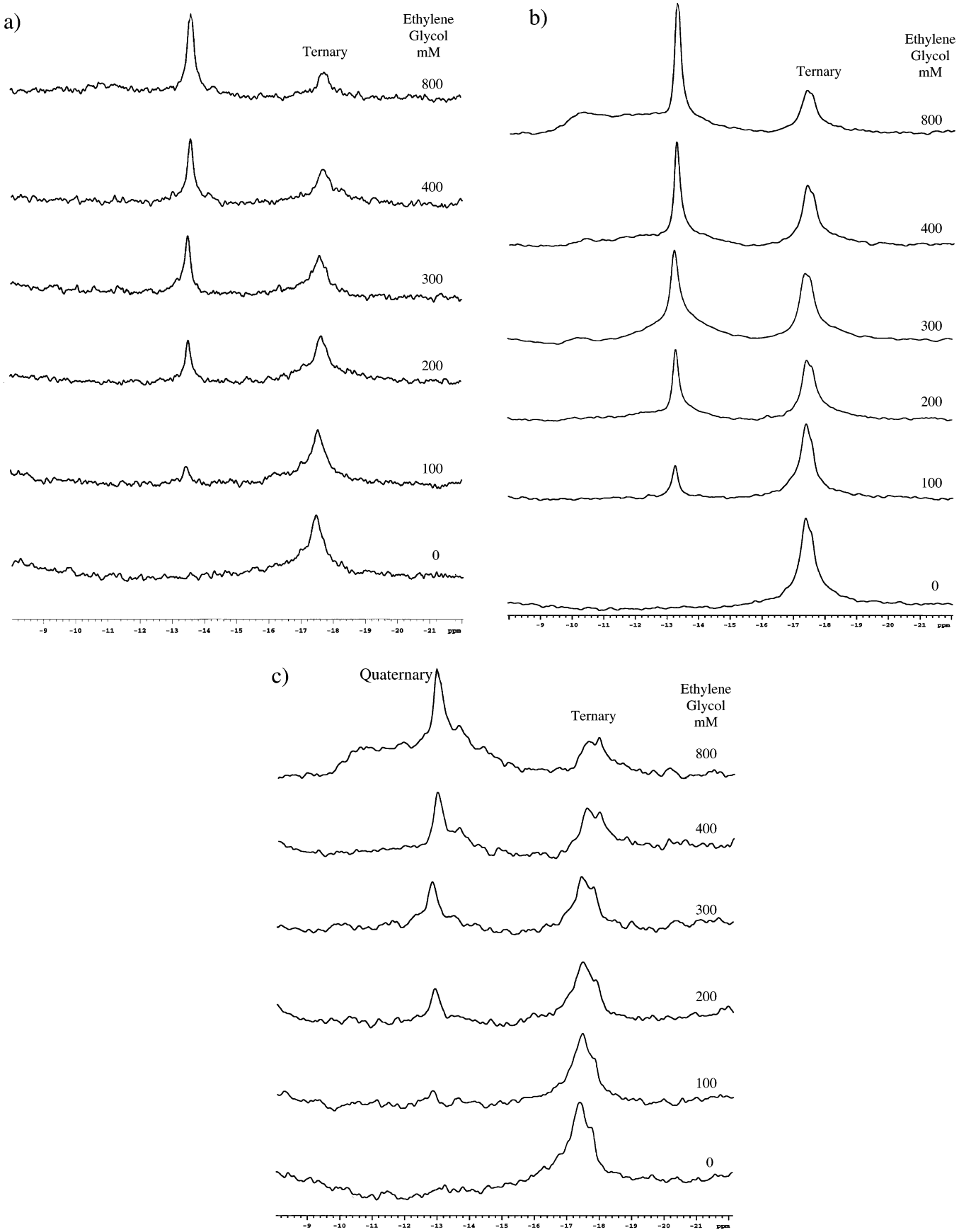

FIGURE 3: ^{11}B NMR spectra obtained on samples containing 2 mM porcine trypsin (type IX), 25 mM borate, and (a) 25 mM G3P; (b) 25 mM 4AM; or (c) 25 mM pHMBA and the ethylene glycol concentrations indicated. The ^{11}B NMR spectra were obtained at 160.6 MHz, 25° C, using a 5-mm quartz NMR tube and a probe which was modified to reduce boron background. The samples also contained 50mM HEPES buffer (pH 8.0). ^{11}B shifts are referenced to external boric acid at pH 4.0. Spectral parameters were sweep width, 10 kHz; acquisition time, 0.6 s; transients, 44,400, for a total acquisition time of 7.4 h. The spectral region containing the ^{11}B resonance of free borate/boric acid at 1.0 ppm is not included in the above figures.

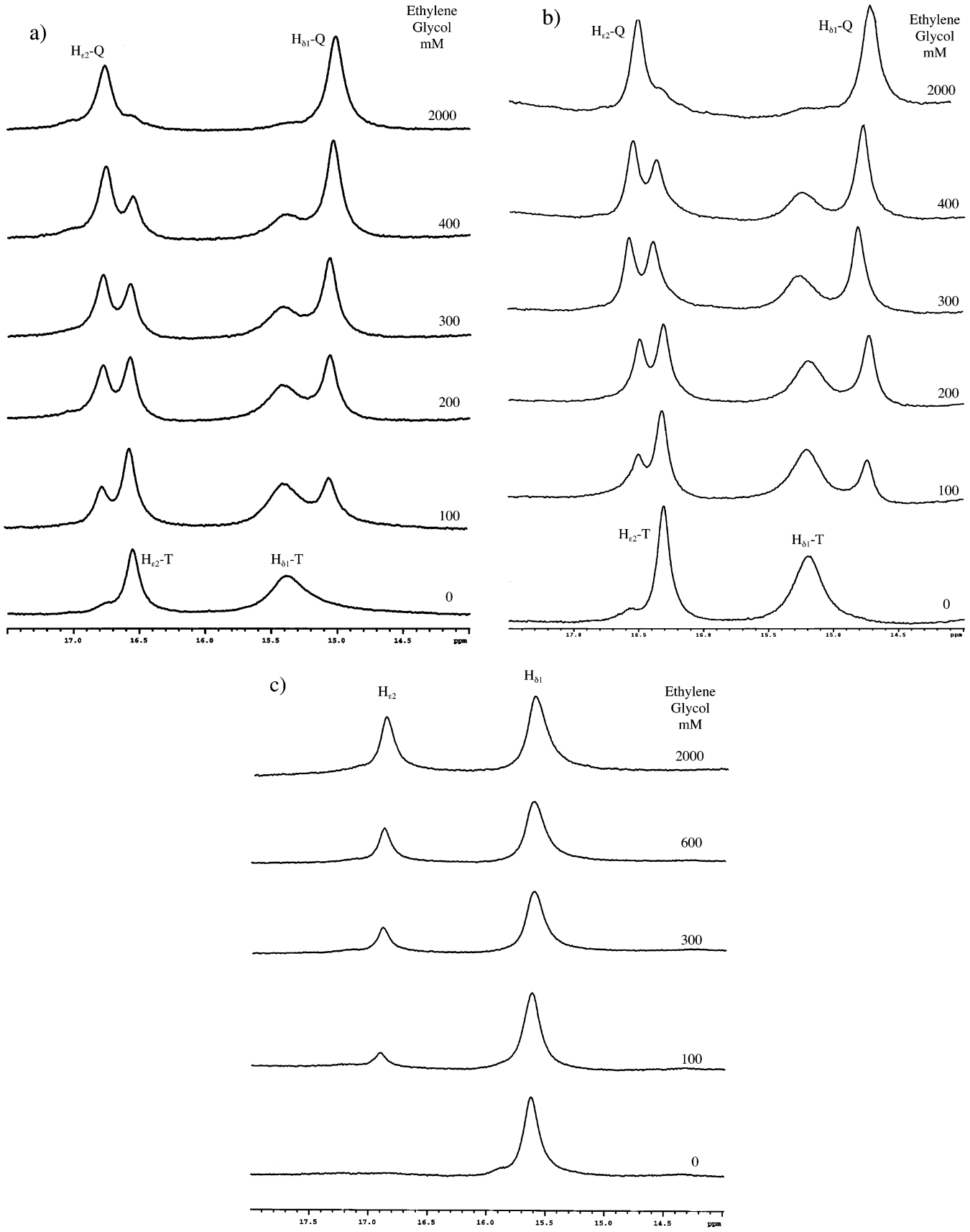

FIGURE 4: ^{1}H NMR spectra showing the His57 resonances of trypsin in the presence of 500 mM borate, and (a) 25 mM G3P; (b) 25 mM 4AB; or (c) 25 mM pHMBA, as a function of added ethylene glycol. The resonances labeled T or Q are assigned to the ternary and quaternary complexes, respectively. The spectra were obtained at 499.9 MHz, 5 °C, on samples containing 2 mM trypsin, 500 mM borate, 100 mM KCl, pH 8.0, 25 mM of either G3P, 4AB, or pHMBA, and the concentrations of EG indicated in the figure. Spectral parameters were: sweep width, 16 kHz; acquisition time, 1.0 s; delay between scans, 1.0 s; transients, 2000, for a total acquisition time of 1.1 h; a jump and return sequence to suppress the H_2O resonance was used (*39*).

Scheme 1

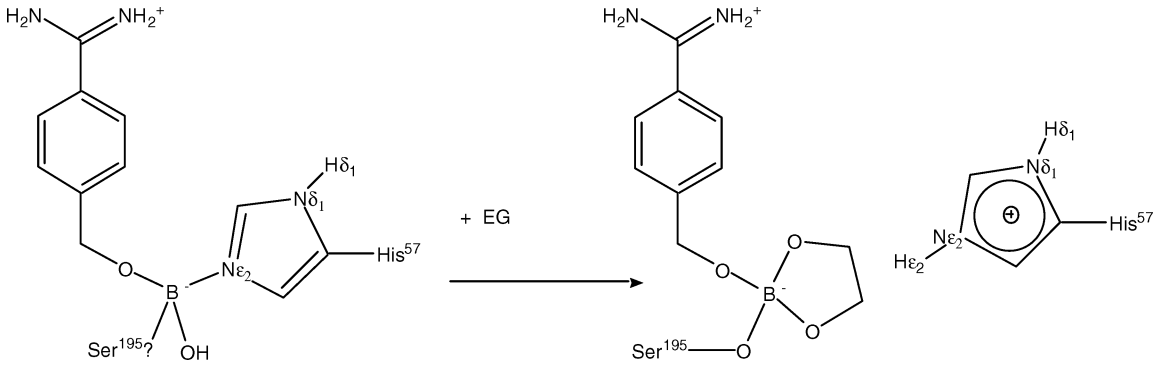

Table 1: Crystallographic Data Summary

Figure 1 reference		*a*	*b*	*c*	*d*	*e*	*f*	*g*	*h*
S1-subsite specific inhibitor		none	none	G3P	G3P	4AB	4AB	*p*HMBA	*p*HMBA
borate soaking	[ ] (mM)	(none)	200	(none)	200	200	200	250	200
	time (min)	(none)	10−20	(none)	2	10−20	10−20	1	10
cryoprotectant		20% EG	20% EG	20% glycerol	20% EG	sat Mg SO_4	20% EG	sat Mg SO_4	20% EG
resolution (Å)		1.7	1.85	1.4	1.8	1.25	1.85	1.45	2.2
R-factor[a] (%)	working	17.6	17.6	17.6	15.5	16.3	15.5	15.4	21.2
	free R[b]	21.6	21.4	18.1	19.8	17.8	17.7	17.9	25.4
completeness (%)		98.0	99.8	89.6	99.8	92.4	99.9	89.1	99.8
redundancy		10.2	6.6	7.5	9.7	7.6	6.6	6.0	8.3
I/σ_I	overall	16.0	21.0	25.1	20.3	21.7	20.6	27.6	20.5
	last shell	8.6	5.6	3.2	4.1	4.2	4.8	4.0	6.4
R-sym[c] (%)	overall	11.9	8.8	5.6	11.9	7.2	9.2	5.1	11.1
	last shell	24.6	36.5	17.1	45.3	35.6	41.1	30.8	37.7
unit cell b dimension (Å)[d]		53.45	55.53	53.45	55.75	53.33	55.77	53.20	55.41
pdb code		1*S*81	1*S*82	1*S*5*S*	1*S*6F	1*S*83	1*S*84	1*S*6H	1*S*85

[a] R-factor $= \sum||F_o| - |F_c||/\sum|F_o|$ calculated from working data set. [b] Free R is calculated from 5% of data randomly chosen not to be included in refinement. [c] Rsym $= \sum(|I_i - \langle I\rangle|)/\sum(I_i)$ where I_i is the intensity of the *i*th observation and $\langle I\rangle$ is the mean intensity of the reflection. [d] Unit cell *a* and *c* dimensions range from 75.7 to 76.4 Å and 46.5 to 46.9 Å, respectively.

boronate inhibitor interacts directly with the His Nϵ2 (possibly in addition to Ser195), so that only the histidine Hδ1 proton is observed (*41*, *43*, *44*). On the basis of the observed crystal structure of the trypsin/*p*HMBA/borate/EG quaternary complex (Figure 1h), addition of EG would be expected to displace the histidine from the borate, so that the four boron ligands are supplied by the trypsin Ser195 oxygen, the *p*HMBA oxygen, and the EG, as shown in Scheme 1.

Examination of the ^{1}H spectrum as a function of EG indicates that the complex observed in the crystal structure (Figure 1h) also forms in solution, with the His57 imidazole side chain gradually converted to an imidazolium cation in which both the Nδ1 and Nϵ2 hydrogen nuclei can be observed (Figure 4c). We note as well that the interpretation given above indicates that the Hδ1 resonance does not shift significantly in going from the ternary to the quaternary complex. In the absence of the EG, the borate may actually bind to the His Nϵ2 or to both His Nϵ2 and Ser195 Oγ, as occurs, for example, in the complex of γ-chymotrypsin with L-*p*-chloro-1-acetamido-boronic acid inhibitor (*45*).

DISCUSSION

Although the structures of many complexes formed from serine proteases and boronate inhibitors have been determined (more than 80 structures of this type are listed in the protein database), the structures reported here provide the first crystallographic evidence for the formation of covalent bonds between borate and protein. While several protein structures containing boric acid or borate molecules have been reported (e.g., ketose reductase (*46*) and xanthine-guanine phosphoribosyl-transferase (*47*)), none to date involves a covalent linkage. The recently reported crystal structure formed from a complex of the bacterial sensor protein LuxP with a furanosyl borate autoinducer contains no covalent bonds between the borate and the protein (*6*). As demonstrated here and in our previous NMR study (*10*), borate complexes can be stabilized by the presence of additional borate ligands that bind to the enzyme and/or stabilize the tetrahedral hybridization of the borate. As noted above, there is substantial indirect evidence for the formation of an analogous ternary complex involving a related enzyme, γ-glutamyl transpeptidase (*12*−*14*). While no direct crystallographic data have been obtained, the construction of a transition state inhibitor, L-2-amino-4-boronobutanoic acid, which mimics the proposed γ-GT/serine/borate structure, provides strong support for the existence of such a ternary complex.

A comparison of the results obtained for the solution and crystalline states provides some unique insights into the formation and stability of the borate complexes. Solution state NMR studies were readily able to identify ternary complexes formed from trypsin, the S1-binding alcohols, and borate; however, similar ternary complexes were not seen in crystals placed in solutions containing as high as 250 mM borate at pH 8. As is apparent from Table 1, formation of active site borate complexes is in all cases accompanied by a significant expansion of the crystal along the *b*-axis. A

more detailed structural evaluation indicates that this expansion parallels a conformational rearrangement, the main feature of which is the extension of the Gln192 side chain in a direction approximately parallel to the crystalline *b*-axis (Figure 2). The data are thus consistent with the conclusion that the complexes formed from borate in the presence of ethylene glycol provide sufficient energy to fuel this conformational rearrangement and the resulting crystal expansion. This in turn suggests that the stability of the ternary complex may be insufficient to overcome the effects of crystal packing, which produce a conformational state characterized by a folded Gln192 side chain which intrudes into the active site. In addition to this effect, sulfate ion, present at 2.0 M concentration when $MgSO_4$ is used as a stabilization solution (and higher concentrations when used as an alternative cryoprotectant), may block the active site. Indeed, the presence of a sulfate ion in the active site is apparent in the structure shown in Figure 1g; however, its occupancy is clearly less than 100%, suggesting that borate binding may not be completely excluded by sulfate. Moreover, the structures in which borate and EG are bound are also determined in the presence of 2.0 M $MgSO_4$, but appear to have 100% occupancy borate/EG bound. This analysis illustrates the value of NMR in providing complementary solution state information for analysis of structures involving weak binding ligands.

The quaternary trypsin/S1-binding alcohol/borate/EG complexes, however, were readily observed both in the solution and crystalline states. For these complexes, the NMR titration data indicate that EG binding is rather weak, requiring very high concentrations of EG to convert from ternary to quaternary forms. However, the quaternary, EG-containing complexes are kinetically more stable, as indicated, for example, by the sharper $^1H\delta1$ resonances for the quaternary complex seen in Figure 4, and by our ability to observe them in the crystalline state. It has been proposed that the catalytic efficiency of the enzyme arises in part from the creation of an oxyanion hole which stabilizes the transition state of the substrate (*48*). In the active site complexes studied here, the oxyanion hole is occupied by borate. Since the bidentate ligation of the EG imposes geometric constraints that strongly favor the tetrahedral, anionic form of borate, EG complexation effectively contributes to the stability of the complex via this electrostatic binding interaction. The ternary trypsin−borate−EG complex observed in the crystalline state is not easily identified in solution, although broadening of the ^{11}B resonances presumably results from an intermediate exchange rate between borate−EG and borate−EG−trypsin complexes. Presumably, the lack of direct interactions between the EG and the enzyme, as well as the competition with 55 M water, explains the difficulty in observing this complex in solution.

In each of the four crystal structures complexed with borate/EG, Ser195 is covalently bound to boron regardless of the presence or absence of an inhibitor in the S1-subsite. Interestingly, NMR studies of trypsin and α-lytic protease have indicated that formation of a binary complex with borate involves binding to His57 Nϵ2 (trypsin), rather than with the Ser195 Oγ (*43*, *44*). One explanation for this difference is the possibility that the interaction of boric acid with histidine requires an addition reaction, while binding of the borate/EG complex with trypsin would involve a substitution

Scheme 2

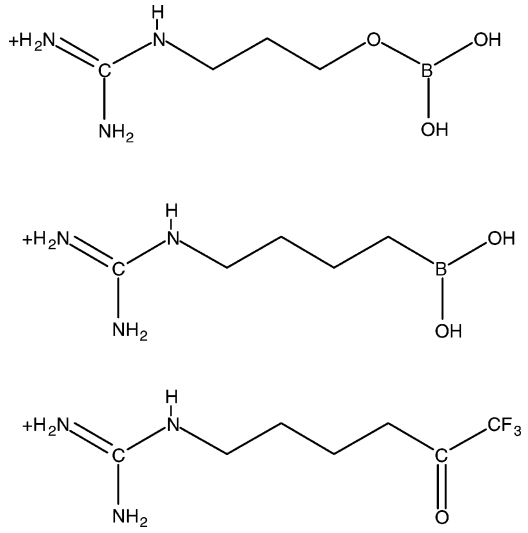

of a hydroxyl ligand by the Ser195 Oγ. The substitution chemistry of borate has been studied by Pizer and co-workers (*49*), and typically requires an incoming ligand, such as a serine hydroxyl, which can donate a proton to a boron-coordinated hydroxyl oxygen to form water, which then acts as a leaving group. In any case, the crystal structure of the trypsin/borate/EG complex indicates that the presence of the EG alters the nature of the complex formed, perhaps as a result of the geometric constraint introduced by the chelation

The present results extend the idea of using enzymes as templates for the organization of simple ligand building blocks into more complex structures. Although such structures have direct implications in terms of the construction of boronate inhibitors, the information derived is not limited to such inhibitors. The alcohols identified in such studies can be combined with other groups capable of binding to the nucleophilic oxygen of serine (*7*, *8*), such as the trifluoromethyl ketone group shown in Scheme 2.

Although the alcohols used for the studies reported were simple substrate analogues predicted to bind to the S1 specificity pocket on the enzyme, different and more complex alcohols could in principle be identified via a screening program or through molecular modeling. The identification of alcohols capable of forming ternary complexes with serine proteases and borate would appear to be a very attractive alternative to a direct evaluation based on the synthesis of boronate inhibitors. The lack of commercially available boronate inhibitors suggests that these are difficult to synthesize. We note also that borate has been found to inhibit other classes of enzymes, and particularly metalloenzymes, e.g., urease (*50*) and arginase (*51*, *52*).[2] Suenaga and co-workers (*27*, *28*) and Katz and co-workers (*29*) have proposed an analogous approach for enhancing the selectivity of boronate derivatives by searching for ternary complexes. In general, the use of boronate ligands as starting points is much more limiting, both in terms of the availability of the boronate ligands and from a structural standpoint. As an illustration of this limitation, the ternary γGT/serine/borate

[2] In ref *51*, the authors discuss a structure of a ternary arginase−borate−ornithine complex in which borate is bound to the manganese cluster, although we were unable to find this structure in the protein data bank.

complex led to the development of a strong inhibitor (*13*, *14*), while studies of ternary alcohol−boronate−γGT complexes (*28*) have not as yet resulted in a significantly improved inhibitor.

The studies reported here provide a particularly striking example of the interaction of crystal packing with active site structure. Formation of four active site complexes was only feasible by forcing a 4% increase in the length of the *b*-axis of the unit cell, within the context of the crystal structures studied. This result has important implications for the use of crystallographic analysis for drug lead discovery (*32*−*34*). The ability of the active site of an enzyme to accommodate ligands that are soaked into a preformed crystal must be considered in light of the subtle constraints imposed by crystal packing. For the case of weakly binding ligands, such constraints may be of paramount importance.

ACKNOWLEDGMENT

The authors are grateful to Dr. Charles Orji of UNIC, LLC for the custom synthesis of the guanidine-3-propanol and the 4-hydroxymethyl benzamidine.

NOTE ADDED AFTER ASAP POSTING

An earlier version of this paper was posted to the ASAP website on February 18, 2004. Additional information on the space group of the trypsin crystals (first sentence under Structural Overview in the Results section) was added to the current version posted February 27, 2004.

SUPPORTING INFORMATION AVAILABLE

Views of the active site that include electron density and other atoms are provided for the eight separate crystal structures. This material is available free of charge via the Internet at http://pubs.acs.org.

REFERENCES

1. Schubert, D. M. (2003) Borates in Industrial Use. *Struct. Bonding 105*, 1−40.
2. Hunt, C. D., and Idso, J. P. (1999) Dietary boron as a physiological regulator of the normal inflammatory response: a review and current research progress. *J. Trace Elem. Exp. Med. 12*, 221−233.
3. Ku, W. W., Chapin, R. E., Wine, R. N., and Gladen, B. C. (1993) Testicular toxicity of boric acid (BA) − relationship of dose to lesion development and recovery in the F344 rat. *Reprod. Toxicol. 7*, 305−319.
4. Gregory, R. B., Rychkov, G., and Barritt, G. J. (2001) Evidence that 2-aminoethyl diphenylborate is a novel inhibitor of store-operated Ca2+ channels in liver cells, and acts through a mechanism which does not involve inositol triphosphate receptors. *Biochem. J. 354*, 285−290.
5. Bilmen, J. G., Wootton, L. L., Godfrey, R. E., Smart, O. S., and Michelangeli, F. (2002) Inhibition of SERCA Ca^{2+} pumps by 2-aminoethoxydiphenyl borate. *Eur. J. Biochem. 269*, 3678−3687.
6. Chen, X., Schauder, S., Potier, N., Van Dorsselaer, A., Pelczer, I., Bassler, B. L., and Hughson, F. M. (2002) Structural identification of a bacterial quorum-sensing signal containing boron. *Nature 415*, 545−549.
7. Walker, B., and Lynas, J. F. (2001) Strategies for the inhibition of serine proteases. *Cellular and Mol. Life Sci. 58*, 596−624.
8. Babine, R. E., and Bender, S. L. (1997) Molecular Recognition of Protein−Ligand Complexes: Application to Drug Design. *Chem. Rev. 97*, 1359−1472.
9. Antonov, V. K., Ivaniva, T. V., Berezin, I. V., and Martinek, K. (1970) *n*-Alkylboronic acids as bifunctional reversible inhibitors of alpha-chymotrypsin. *FEBS Lett. 16*, 23−25.
10. London, R. E., and Gabel, S. A. (2002) Formation of a Trypsin-Borate-4-Aminobutanol Ternary Complex. *Biochemistry 41*, 5963−5967.
11. Revel, J. P., and Ball, E. G. (1959) The reaction of glutathione with amino acids and related compounds as catalyzed by gamma-glutamyl transpeptidase. *J. Biol. Chem. 234*, 577−582.
12. Tate, S. S., and Meister, A. (1978) Serine-borate complex as a transition-state inhibitor of gamma-glutamyl transpeptidase. *Proc. Natl. Acad. Sci. U.S.A. 75*, 4806−4809.
13. London, R. E., and Gabel, S. A. (2001) Development and Evaluation of a Boronate Inhibitor of γ-Glutamyl Transpeptidase. *Arch. Biochem. Biophys. 385*, 250−258.
14. Stein, R. L., DeCicco, C., Nelson, D., and Thomas, B. (2001) Slow-binding inhibition of gamma-glutamyl transpeptidase by gamma-boroGlu. *Biochemistry 40*, 5804−5811.
15. Griffith, O. W., and Meister, A. (1979) *Proc. Natl. Acad. Sci. U.S.A. 76*, 268−272.
16. Siao, C. J., and Tsirka, S. E. (2002) Extracellular proteases and neuronal cell death. *Cell. Mol. Biol. 48*, 151−161.
17. Wolf, B. B., and Green, D. R. (2002) Apoptosis: Letting slip the dogs of war. *Curr. Biol. 12*, R177−R179.
18. Kilian, M., Reinholdt, J., Lomholt, H., Poulsen, K., and Frandsen, E. V. G. (1996) Biological significance of IgA1 proteases in bacterial colonization and pathogenesis: Critical evaluation of experimental evidence APMIS. *104*, 321−338.
19. Lahm, A., Yagnik, A., Tramontano, A., and Koch, U. (2002) Hepatitis C virus proteins as targets for drug development: The role of bioinformatics and modeling. *Curr. Drug Targets 3*, 281−296.
20. Webber, M. M., Waghray, A., and Bello, D. (1995) Prostate-specific antigen, a serine protease, facilitates human prostate cancer cell invasion *Clin. Cancer Res. 1*, 1089−1094.
21. Rao, C. N., Lakka, S. S., Kin, Y, Konduri, S. D., Fuller, G. N., Mohanam, S., and Rao, J. S. (2001) Expression of tissue factor pathway inhibitor 2 inversely correlates during the progression of human gliomas. *Clin. Cancer Res. 7*, 570−576.
22. Mitsudo, K., Jayakumar, A., Henderson, Y., Frederick, M. J., Kang, Y., Wang, M., El-Naggar, A. K., and Clayman, G. L. (2003) Inhibition of serine proteinases plasmin, trypsin, subtilisin A, cathepsin G, and elastase by LEKTI: a kinetic analysis. *Biochemistry 42*, 3874−3881.
23. Riewald, M., and Ruf, W. (2002) Orchestration of coagulation protease signaling by tissue. *Trends Cardiovasc. Med. 12*, 149−154.
24. Collen D., and Lijnen, H. R. (1991) in *Hematology Basic Principles and Practice* (Hoffman, R., Benz, E. J., Jr., Shattil, S. J., Furie, B., and Cohen, H. J., Eds.) pp 1232−1242, Churchill Livingstone, NY.
25. Fleischer, B. (1994) CD26 − A surface protease involved in T-cell activation. *Immunol. Today 15*, 180−184.
26. Arlaud, G. J., Gaboriaud, C., Thielens, N. M., and Rossi, V. (2002) Structural biology of C1. *Biochem. Soc. Transact. 30*, 1001−1006.
27. Suenaga, H., Mikami, M., Yamamoto, H., Harada, T., and Shinkai, S. (1995) Strong inhibitory effect of sugar biphenylboronic acid complexes on the hydrolytic activity of α-chymotrypsin. *J. Chem. Soc., Perkin Trans. 1*, 1733−1738.
28. Suenaga, H., Nakashima., K, Mikami., M, Yamamoto, H., James, T. D., Sandanayake, K. R. A. S., and Shinkai, S. (1996) Screening of arylboronic acids to search for a strong inhibitor for gamma-glutamyl transpeptidase (gamma-GTP) *Recl. Trav. Chim. Pays-Bas 115*, 44−48.
29. Katz, B. A., Finer-Moore, J., Mortezaei, R., Rich, D. H., and Stroud, R. M. (1995) Episelection: Novel $K_i \sim$ nanomolar ilnhibitors of serine proteases selected by binding or chemistry on an enzyme surface. *Biochemistry 34*, 8264−8280.
30. Shuker, S. B., Hajduk, P. J., Meadows, R. P., and Fesik, S. W. (1996) Discovering high-affinity ligands for proteins: SAR by NMR. *Science 274*, 1531−1534.
31. Li, D., and London, R. E. (2002) Ligand discovery using the inter-ligand Overhauser effect: horse liver alcohol dehydrogenase. *Biotechnol. Lett. 24*, 623−629.
32. Blundell, T. L., Jhoti, H., and Abell, C. (2002) High-throughput crystallography for lead discovery in drug design. *Nat. Rev. Drug Discuss. 11*, 45−54.
33. Carr, R., and Jhoti, H. (2002) Structure-based screening of low-affinity compounds. *Drug Discov. Today 7*, 522−527.
34. Blundell, T. L., Abell, C., Cleasby, A., Hartshorn, M. J., Tickle, I. J., Parasini, E., and Jhoti, H. (2002) High-Throughput X-ray

Crystallography for Drug Discovery in *Drug Design: Cutting Edge Approaches* (Flower, D. R., Ed.), pp 53−59, Royal Society of Chemistry, Cambridge, U.K.
35. Otwinowski, Z., and Minor, W. (1997) Processing of X-ray Diffraction Data Collected in Oscillation Mode in *Methods in Enzymology Vol. 276: Macromolecular Crystallography, Part A,* Carter, C. W., Jr., and Sweet, R. M., Eds., pp 307−326, Academic Press, New York.
36. Johnson, A., Krishnaswamy, S., Sundaram, P. V., and Pattabhi, V. (1997) The first structure at 1.8 angstrom resolution of an active autolysate form of porcine alpha-trypsin. *Acta Crystallogr. D Biol. Crystallogr. 53*, 311−315.
37. Brunger, A. T., Adams, P. D., Clore, G. M., Delano, W. L., Gros, P., Grosse-Kunsteleve, R. W., Jiang, J.-S., Kuszewski, J., Nilges, N., Pannu, N. S., Read, R. J., Rice, L. M., Simonson, T., and Warren, G. L. (1998). Crystallography and NMR System (CNS): A New Software System for Macromolecular Structure Determination. *Acta Crystallogr. D54*, 905−921.
38. Cornell, W. D., Cieplak, P., Bayly, C. I., Gould, I. R., Merz, K. M., Ferguson, D. M., Spellmeyer, D. C., Fox, T., Caldwell, J. W., and Kollman, P. A. (1995) A 2nd generation force-field for the simulation of proteins, nucleic-acids, and organic-molecules. *J. Am. Chem. Soc. 117*, 5179−5197.
39. Plateau, P., and Gueron, M. (1982) Exchangeable proton NMR without baseline distortion, using new strong pulse sequences. *J. Am. Chem. Soc. 104*, 7310−7311.
40. Tsunematsu, H., Imamura, T., and Makisumi, S. (1983) Kinetics of hydrolysis of Na-benzoyl-*p*-guanidino-L-phenylalanine *p*-nitroanilide by Trypsin. *J. Biochem. (Tokyo) 94*, 123−128.
41. Tsilikounas, E., Kettner, C. A., and Bachovchin, W. W. (1992) Identification of serine and histidine adducts in complexes of trypsin and trypsinogen with peptide and nonpeptide boronic acid inhibitors by ^{1}H NMR spectroscopy. *Biochemistry 31*, 12651−12655.
42. Coddington, J. M., and Taylor, M. J. (1989) High field ^{11}B and ^{13}C NMR investigations of aqueous borate solutiosn and borate-diol complexes. *J. Coord. Chem. 20*, 27−38.
43. Tsilikounas, E., Kettner, C. A., and Bachovchin, W. W. (1993) ^{11}B NMR spectroscopy of peptide boronic acid inhibitor complexes of α-lytic protease. Direct evidence for tetrahedral boron in both boron-histidine and boron-serine adduct complexes. *Biochemistry 32*, 12651−12655.
44. Bachovchin, W. W., Wong, W. Y. L., Farr-Jones, S., Shenvi, A. B., and Kettner, C. A. (1988) N-15 NMR spectroscopy of the catalytic triad histidine of a serine protease in peptide boronic acid inhibitor complexes. *Biochemistry 27*, 7689−7697.
45. Stoll, V. S., Eger, B. T., Hynes, R. C., Martichonok, V., Jones, J. B., and Pai, E. F. (1998) Differences in binding modes of enantiomers of 1-acetamido boronic acid based protease inhibitors: crystal structures of gamma-chymotrypsin and subtilisin Carlsberg complexes. *Biochemistry 37*, 451−462.
46. Banfield, M. J., Salvucci, M. E., Baker, E. N., and Smith, C. A. (2001) Crystal Structure of NADP(H)-Dependent Ketose Reductase from *Besimia Argentifolii* at 2.3 Angstrom Resolution. *J. Mol. Biol. 306*, 239−250.
47. Vos, S., Parry, R. J., Burns, M. R., De Jersey, J., and Martin, J. L. (1998) Structures of Free and Complexed Forms of Escherichia Coli Xanthine-Guanine Phosphoribosyltransferase. *J. Mol. Biol. 282*, 875−889.
48. Menard, R., and Storer, A. C. (1992) Oxyanion hole interactions in serine and cysteine proteases. *Biol. Chem. Hoppe-Seyler 373*, 393−400.
49. Babcock, L., and Pizer, R. (1980) Dynamics of boron acid complexation reactions − formation of 1−1 boron acid ligand complexes. *Inorg. Chem. 19*, 56−61; Pizer, R., and Selzer, R. (1984) The boric acid lactic acid system − equilibria and reaction mechanism. *Inorg. Chem. 23*, 3023−3026; Pizer, R., and Ricatto, P. J. (1994) Thermodynamics of several 1−1 and 1−2 complexation reactions of the borate ion with bidentate ligands − B-11 NMR spectroscopic studies. *Inorg. Chem. 33*, 2402−2406.
50. Breitenbach, J. M., and Hausinger, R. P. (1988) *Proteus mirabilis* urease, Partial purification and inhibition by boric acid and boronic acids. *Biochem. J. 250*, 917−920.
51. Baggio, R., Elbaum, D., Kanyo, Z. F., Carroll, P. J., Cavalli, R. C., Ash, D. E., and Christianson, D. W. (1997) Inhibition of Mn2-(2+)-Arginase by borate leads to the design of a transition state analogue inhibitor, 2(S)-Amino-6-boronohexanoic acid. *J. Am. Chem. Soc. 119*, 8107−8108.
52. Cama, E., Colleluori, D. M., Emig, F. A., Sin, H., Kim, S. W., Kim, N. N., Traish, A. M., Ash, D. E., and Christianson, D. W. (2003) Human arginase II: crystal structure and physiological role in male and female sexual arousal. *Biochemistry 42*, 8445−8451.

BI035782Y